Cornea

A Mathematical Model of Corneal Metabolism in the Presence of an Iris-Fixated Phakic Intraocular Lens

Peyman Davvalo Khongar,[1] Jan O. Pralits,[1] Xi Cheng,[2] Peter Pinsky,[2] Paolo Soleri,[3] and Rodolfo Repetto[1]

[1]Department of Civil, Chemical and Environmental Engineering, University of Genoa, Genoa, Italy
[2]Mechanical Engineering, Stanford University, Stanford, California, United States
[3]Ophtec BV, Groningen, The Netherlands

PURPOSE. Corneal endothelial cell loss is one of the possible complications associated with phakic iris-fixated intraocular lens (PIOL) implantation. We postulate that this might be connected to the alteration of corneal metabolism secondary to the lens implantation.

METHODS. A mathematical model of transport and consumption/production of metabolic species in the cornea is proposed, coupled with a model of aqueous flow and transport of metabolic species in the anterior chamber.

RESULTS. Results are presented both for open and closed eyelids. We showed that, in the presence of a PIOL, glucose availability at the corneal endothelium decreases significantly during sleeping.

CONCLUSIONS. Implantation of a PIOL significantly affects nutrient transport processes to the corneal endothelium especially during sleep. It must still be verified whether this finding has a clinical relevance.

Keywords: aqueous flow, corneal endothelial cells, intraocular lens, nutrient transport, mathematical model

In recent years, phakic iris-fixated intraocular lenses (PIOLs) have attracted widespread acceptance for refractive error correction and, in particular, for treating myopia. PIOLs are surgically implanted in the anterior chamber of the eye and fixated to the iris by haptics. Recent developments in lens manufacturing technologies, design, and surgical procedures have significantly decreased the risk of complications associated with PIOL implantation, and PIOLs are generally considered very safe. In some cases, a decrease in corneal endothelial cell density has been observed after PIOL implantation,[1,2] although this finding is still under debate and some authors have not observed evidence of it.[3]

Various mechanisms have been proposed and investigated to explain the possible occurrence of corneal endothelium cell loss in the presence of PIOLs. The surgical procedure itself can cause a decrease in endothelial cell density. Mechanical friction between the endothelium and the PIOL has also been postulated to possibly cause cell detachment in patients with the habit of rubbing their eyes or sleeping face down. Various authors[4–6] have investigated through mathematical models the possible role of changes in the wall shear stress on the cornea due to aqueous humor motion on endothelial cell detachment. The authors have found that implantation of a PIOL does not induce a significant increase of the stress on the cornea and thus this is unlikely to cause cell loss.

Repetto et al.[4] and Davvalo Khongar et al.[7] have postulated that cell loss could be associated with a decrease in nutrient availability at the corneal endothelium in the presence of a PIOL. Since the cornea is an avascular tissue it relies on oxygen and nutrient supply from the surrounding tissues or from the external environment. In the healthy cornea, oxygen is primarily supplied by the surrounding air when the eyelids are open and from blood circulation in the palpebral conjunctiva when the eyelids are closed.[8] On the other hand, glucose primarily diffuses into the cornea from the aqueous humor.[9] The hypothesis put forward in the studies by Repetto et al.[4] and Davvalo Khongar et al.[7] is that the presence of a PIOL may interfere with the delivery of nutrients to the cornea. In particular, when the eyelids are open, owing to the existence of a temperature gradient across the anterior chamber, a buoyancy-driven aqueous flow is generated that quite efficiently allows mixing of the aqueous in the anterior chamber.[10] This flow also exists with a similar intensity in the presence of a PIOL.[4,11] Moreover, daytime eye rotations also generate significant velocities and mixing in the aqueous.[11,12] Thus, in this case the presence of the PIOL is not likely to interfere much with nutrient transport to the cornea. On the other hand, during sleep the eyelids are closed and, when rapid eye movements (REMs) do not occur, the eye globe is approximately fixed. In this case both of the above flows are suppressed and the only mechanism generating fluid flow in the anterior chamber is aqueous production at the ciliary processes. The presence of a PIOL diverts the flow passing through the pupil toward the periphery of the anterior chamber and effectively shields the central cornea. In fact, the flow anterior to the PIOL is very slow in this case[4] and nutrients have to rely mostly on molecular diffusion to reach the central region of the corneal epithelium, which is a very inefficient transport mechanism, on the spatial scale of millimeters. Thus during eyelid closure the cornea might experience nutrient depletion in the presence of a PIOL.

2311

The aim of the present work was to explore this hypothesis. To this end we developed a mathematical model that accounts for aqueous flow in the anterior chamber and reaction-diffusion metabolic processes in the cornea.

Several mathematical models[8,13–16] and experiments[17–21] have been proposed, aimed at describing corneal metabolism. Taking advantage of the fact that the thickness of the cornea is much smaller than its lateral dimension, in most cases one-dimensional models have been adopted in which the transport of all species across the cornea is assumed to be much larger than in the other directions. Chhabra et al.[14] have proposed a coupled reaction-diffusion model for nutrient and oxygen delivery to the cornea, which together with the model proposed by Pinsky,[15] is the basis of the model used in this work. None of the above works have considered the direct effect of aqueous flow in delivering nutrients to the cornea.

## MATERIALS AND METHODS

Corneal Metabolism Model

Glucose consumption from corneal cells occurs through two main pathways: aerobic (or tricarboxylic acid or Krebs cycle) and anaerobic (Embden-Meyerhof) glycolysis.[22] For the normal rabbit cornea, $\approx 15\%$ of glucose breakdown is through aerobic glycolysis.[23,24] Moreover, only $\approx 10\%$ of corneal glucose is supplied from glycogen and endogenous glucose.[23] The latter contribution was neglected in this work.

In glycolysis, one mole of 6-carbon glucose is first converted into 3-carbon pyruvate. Then, in the presence of oxygen, pyruvate is converted to acetyl-CoA and enters the Krebs cycle, resulting in the formation of carbon dioxide and, through oxidative phosphorylation, water. This pathway is simplified as follows:

$$C_6H_{12}O_6 + 6O_2 \rightarrow 6CO_2 + 6H_2O + \text{energy}. \quad (1)$$

In aerobic respiration, 6 moles of water and 6 moles of carbon dioxide are produced by the consumption of 1 mole of glucose with 6 moles of oxygen and the reaction produces 36 net moles of adenosine triphosphate (ATP).[23,24]

In the absence of oxygen, the pyruvate produced by glycolysis is converted to lactate and hydrogen ions. This pathway is called Embden-Meyerhof and is simplified as follows:

$$C_6H_{12}O_6 \rightarrow 2C_3H_5O_3^- + 2H^+ + \text{energy}. \quad (2)$$
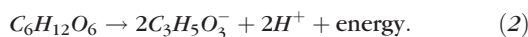
In this path, for each mole of consumed glucose, 2 moles of ATP are produced. Acidification of the cornea due to this reaction is buffered by bicarbonate ion to produce dissolved carbon dioxide.

Transport Equations

As described in the previous section, corneal metabolism relies on the availability of oxygen and nutrients. Proper functioning of the metabolic processes described above is essential for corneal health. For example, accumulation of lactate ions due to lack of oxygen tension leads to edema.[16,25] In this article, following Pinsky,[15] we only considered the following three metabolic species: oxygen, glucose, and lactate.

As discussed in the introduction, when the eyelids are open the thermally driven buoyancy flow and eye rotations quite effectively mix the aqueous in the anterior chamber, smoothing out concentration gradients. This allowed us to avoid solving the problem of aqueous motion and transport in the anterior chamber. Rather, we assumed that concentration of all species is uniformly distributed in the anterior chamber and just imposed the corresponding concentration values as boundary conditions on the endothelium when solving the problem in the cornea.

On the contrary, when the eyelids are closed, aqueous velocities are much smaller and concentration gradients can develop in the anterior chamber. This implies that in order to study metabolic species transport to the cornea in this case, it is necessary to account for aqueous motion in the anterior chamber. This ingredient is essential for understanding the possible role of the presence of a PIOL.

We modeled the aqueous humor as an incompressible, Newtonian fluid. Fluid motion is governed by the Navier-Stokes and continuity equations that read as follows:

$$\frac{\partial \mathbf{u}}{\partial t} + (\mathbf{u} \cdot \nabla)\mathbf{u} + \frac{1}{\rho}\nabla p - \nu\nabla^2\mathbf{u} = \mathbf{0}, \quad (3a)$$

$$\nabla \cdot \mathbf{u} = 0, \quad (3b)$$

where t is time, $\mathbf{u}$ denotes the velocity vector, p is the departure of the pressure from the hydrostatic profile (thus we omit the gravitational acceleration), ρ is the density, and ν is the kinematic viscosity. The values of the density and viscosity adopted in the simulations are reported below.

Transport of metabolic species in the anterior chamber is governed by the advection/diffusion equation

$$\frac{\partial c_i}{\partial t} + (\mathbf{u} \cdot \nabla)c_i - D_i^{aq}\nabla^2 c_i = 0 \qquad (i = O, G, L). \quad (4)$$

In the above equation subscripts $i = O$, G, and L refer to oxygen, glucose, and lactate ion, respectively. c_i and D_i^{aq} are the concentration and diffusion coefficients of the corresponding metabolic species in aqueous, respectively. In our model the oxygen concentration c_O will be represented as $k_O\, p_O$ where k_O is Henry's constant for oxygen ($k_O = 1.283 \times 10^{-5}$ mM/Pa) and p_O is the oxygen tension.

Chhabra et al.[14] have proposed a one-dimensional metabolic model for the corneal layers, which is generalized to three dimensions by Pinsky.[15] Transport of oxygen, glucose, and lactate ion in the corneal layers is governed by the following diffusion/reaction equations:

$$\frac{\partial c_i}{\partial t} - D_i^j\nabla^2 c_i + mQ_i^j = 0 \qquad (i = O, G, L). \quad (5)$$

In the above equations, the index j refers to the three corneal layers of endothelium, stroma, and epithelium. $Q_i^j (i = O, G, L)$ refers to oxygen, glucose consumption, and lactate production rate in each corneal layer j, respectively. Moreover, m is 1 for oxygen and glucose (consumption) and -1 for lactate ion (production). D_i^j refers to the diffusion coefficients of metabolic species i, for each corneal layer, see Table 1.

Reaction Models

In Chhabra et al.[14] and Pinsky,[15] for each layer of the cornea the dependency of Q_O^j on both p_O and c_G is modeled by using an enzymatic Monod kinetics model. We modified the authors' approach and used a sigmoidal function to model the dependency of Q_O^j on p_O, as proposed by Alvord et al.[13] The reason for this choice is that a sigmoidal function better fits the in vivo experiments of Bonanno et al.[26] This results in the use of the following expression for the oxygen consumption rate:

$$Q_O^j = \frac{Q_{Omax}^j}{1 + e^{\frac{-(p_O - p_{crit})}{R}}}\frac{c_G}{c_G + K_G^O}\left(1 + 0.8\frac{7.6 - pH}{K_{pH} + 7.6 - pH}\right). \quad (6)$$

The parameters appearing in the sigmoidal function are based on the experimental data of Bonanno et al.[26] and

TABLE 1. Parameters Used in Equations 5 and 6

Corneal Properties 1				
Parameter	Units	Endothelium	Stroma	Epithelium
$D_O^j k_O$	Barrer	5.3	29.5	18.8
D_G^j	10^{-6} cm^2/s	3.0	3.0	3.0
D_L^j	10^{-6} cm^2/s	4.4	4.4	4.4
Q_{Omax}^j	10^{-5} mL O$_2$/mL/s	47.78	2.29	25.9

All values from Pinsky.[15]

reported in Table 2.[13,14,22] The glucose Monod dissociation equilibrium K_G^O is considered equal to 0.4 mm Hg, corresponding to an oxygen consumption rate of 93.75% of the saturation value at a glucose concentration of 6 mM.[14] The third term inside the brackets of Equation (6) refers to the reduction of pH from the normal value of 7.6 due to acidosis, which is described in Chhabra et al.[14] In the case of open eyelids, corneal pH is approximately 7.6, while when the eyelids are closed, it decreases to approximately 7.39.[18] Glucose consumption and lactate ion production have the same expressions as proposed by Chhabra et al.[14]

Geometry

Figure 1 represents the idealized axisymmetric shape of the anterior chamber and the cornea. Following Repetto et al.,[4] we neglected the flow in the posterior chamber. Thus the iris-lens channel represents the inlet section of the production/drainage flow used in the simulations related to closed eyelids. The cornea consists of three layers, namely, endothelium, stroma, and epithelium, moving inside out (Fig. 1, inset). The Descemet's and Bowman's membranes are considered part of the stroma, since they have similar transport properties.[8] Geometric characteristics of the cornea are given in Table 3.[4,15,27]

We performed simulations, with and without a PIOL. For the PIOL we considered the Artiflex lens, whose geometry was provided by the manufacturer (Ophtec BV, Groningen, The Netherlands). In all simulations we neglected the presence of the PIOL haptics, which were shown in Repetto et al.[4] to have a negligible influence on aqueous flow. We also studied the effect of a perforation with a diameter of 0.36 mm in the center of the body of the PIOL.

Since both the geometry of the anterior chamber and that of the Artiflex (without haptics) are axisymmetric, the resulting geometry is also axisymmetric, which allowed us to solve an axisymmetric problem on a plane.

We note that in the present work we neglected the presence of an iridotomy, that is, a perforation in the iris, which is typically performed when iris-fixated lenses are implanted and whose role on the fluid dynamics in the anterior chamber in the presence of a PIOL has been investigated by Fernández-Vigo et al.[6,28]

TABLE 2. Parameters Used in Equations 5 and 6

Corneal Properties 2		
p_{crit}	40.9 mm Hg	Alvord et al.[13]
R	13 mm Hg	Alvord et al.[13]
Corneal pH (open eyelids)	7.6	Harvitt and Bonanno[20]
Corneal pH (closed eyelids)	7.39	Harvitt and Bonanno[20]
K_{pH}	0.1	Chhabra et al.[14]
K_G^O	0.4 mM	Chhabra et al.[14]

TABLE 3. Geometrical Parameter Values of the Anterior Chamber and Cornea Used in the Simulations

Geometric Characteristics of the Anterior Chamber		
Diameter	≈13 mm	Repetto et al.[4]
Maximum height	2.63 mm	von Helmholtz[27]
Minimum radius of curvature of the cornea	6.8 mm	von Helmholtz[27]
Radius of curvature of the lens	10 mm	von Helmholtz[27]

Geometric Characteristics of the Cornea		
Endothelium thickness	0.005 mm	Pinsky[15]
Stroma thickness	0.5 mm	Pinsky[15]
Epithelium thickness	0.05 mm	Pinsky[15]

Boundary Conditions

We performed two series of simulations: with open and with closed eyelids. The open eyelids simulations are meant to validate the model, since many clinical observations are available for this case.

Open Eyelids

At the interfaces between each corneal layer, the three metabolic species should satisfy continuity of concentrations. Moreover, conservation of mass requires continuity of normal fluxes. Oxygen tension, glucose concentration, and lactate ion concentration at the anterior chamber–endothelium interface are set at 24 mm Hg, 6.9 mM, and 7.7 mM, respectively.[14] At the epithelium–tear film interface, the oxygen tension is set at 155 mm Hg, which corresponds to the atmospheric oxygen tension.[14] Glucose and lactate fluxes at the interface between the tear film and the anterior chamber is set to zero.[14,15] At the corneal limbus, we consider a zero flux boundary condition for all metabolic species.[14,15]

Closed Eyelids

The measurement of oxygen tension in the anterior chamber is crucial when specifying the boundary conditions for the validation of our models. We mainly focused our attention on the article by McLaren et al.[21] in which the authors use a scanning ocular fluorometer and measure the oxygen tension through the depth of the anterior chamber. This experiment was repeated for different cases and we focused our attention on the measurement of oxygen tension obtained on the cornea in the case with a PMMA contact lens and when eyelids are closed. Most of the oxygen is provided to the cornea from the air, with open lids, and from the palpebral conjunctiva, with closed lids. Since the oxygen permeability of a PMMA contact lens is low, a very small amount of oxygen can pass through it and thus the cornea is deprived of these oxygen sources. In this case, we speculate that oxygen is mostly provided by the aqueous humor. Under these conditions, McLaren et al.[21] have found that the oxygen tension close to the crystalline lens is approximately equal to 6 mm Hg and it decreases to 3 mm Hg in the central region of the anterior chamber. Following these observations, we set the oxygen tension on the crystalline lens and the inlet channel to 6 mm Hg. At these surfaces, we imposed a lactate ion concentration equal to 9 mM.[29] Concerning glucose concentration, the choice is not obvious. In the open eyelids case, assuming that concentration gradients in the anterior chamber are smoothed out by aqueous motion, we assumed a value of 6.9 mM directly at the corneal endothelium. In the case of closed eyelids we need glucose
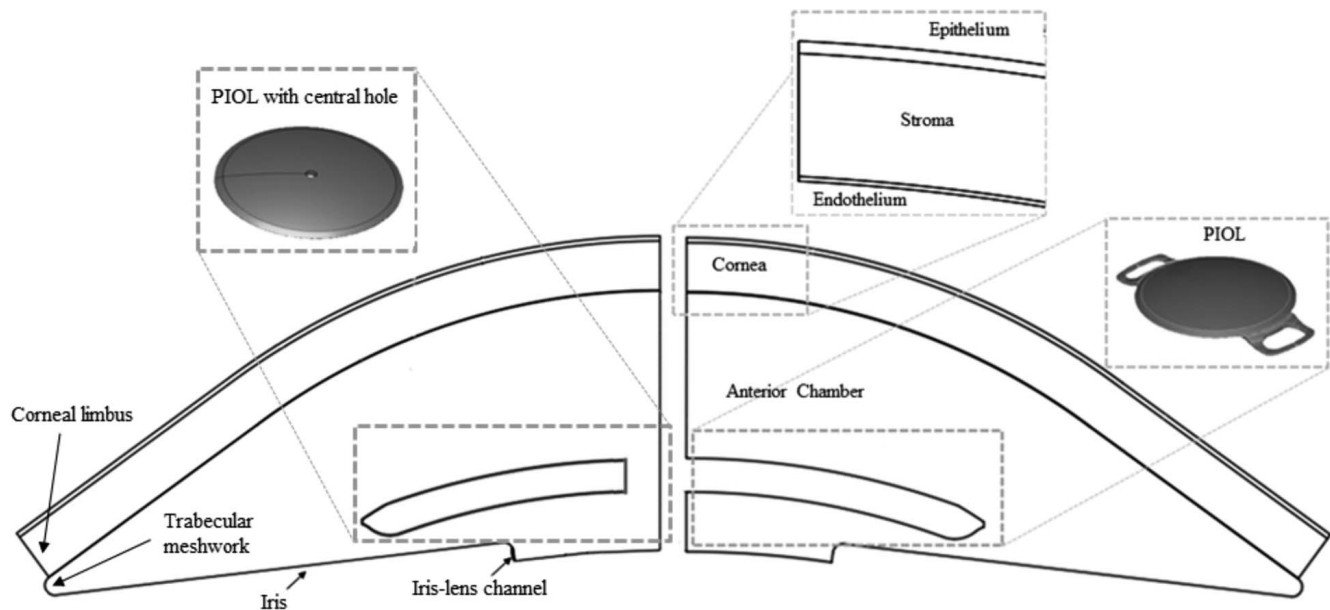
FIGURE 1. Cross-section of the idealized anterior chamber with corneal layers and implanted PIOL. *Left*: PIOL with a central perforation. *Right*: PIOL without perforation.

concentration in the aqueous at the iris-lens channel, which is the inlet of the domain. The value of 6.9 mM can be seen as a lower limit value: any values smaller than this would necessarily produce a smaller value at the corneal endothelium, which would be inconsistent with the condition used for the open eyelids case. On the other hand an upper limit for glucose concentration in the aqueous humor is the glucose concentration in blood at the ciliary processes (8.3 mM),[30] where the aqueous is secreted. Following the above reasoning, we tried different values in the range 6.9 mM to 8.3 mM. The actual value adopted is relevant if one wishes to compare the open and closed eyelid cases. However, we note that it is less crucial when comparing the cases with and without the PIOL, which is the main focus of the present work. This is because for the latter comparison all simulations will be run for the closed eyelids case. As baseline in the following, we used the value of 7.5 mM for glucose concentration at the crystalline lens and the iris-lens channel.

For the iris and corneal limbus, we imposed zero flux for all metabolic species. At the epithelium–tear film interface, since information regarding fluxes are absent in the literature, the oxygen tension was set to 61.5 mm Hg, which is the oxygen tension in the palpebral conjunctiva.[14] In analogy with the open eyelids case, glucose and lactate fluxes were set to zero at the epithelium–tear film interface. At the trabecular meshwork, an outflow boundary condition (zero diffusive flux) for all of the metabolic species was imposed.

For aqueous flow, at the iris-lens channel we imposed a parabolic velocity profile, which corresponds to a volumetric flux Q across the patch equal to 2.5×10^{-11} m³/s (Table 4).[31–33] Aqueous production is known to vary from diurnal to nocturnal conditions; the value we assumed is close to what Nau et al.[34] have found for the latter case ($\approx 2.2 \times 10^{-11}$ m³/s). At the trabecular meshwork zero pressure is imposed, thus the pressure has to be interpreted as the departure from the value at the trabecular meshwork. We assumed that all other surfaces are solid walls and imposed a so-called no-slip boundary condition.

We solved the governing equations with the associated boundary conditions, using Comsol Multiphysics version 4.3a (Stockholm, Sweden).

RESULTS

We first studied the steady state solution of the problem described in the previous section and we then investigated the time required for this steady solution to be reached, starting from a given initial condition. For all cases, we ran a simulation both with and without the PIOL. We also investigated the effect of a perforation in the PIOL[5] on the transport of metabolic species in the anterior chamber and cornea. The first REM phase occurs approximately 90 minutes after falling asleep, but this was not explicitly modeled here. However, our unsteady simulations reproduced the evolution of glucose and lactate concentrations and oxygen tension, before the first REM phase starts. Further, the steady solutions provided the aforementioned values in the limit of long sleep phases without REM.

Steady Simulations

Solution in the Absence of PIOL. Figure 2 shows the steady state profiles of oxygen tension (Fig. 2a) and of lactate (Fig. 2b) and glucose (Fig. 2c) concentration across the thickness of the axis of symmetry of the cornea. In the plots the *x*-axis represents a coordinate in the direction toward the anterior pole, with the origin at the interface between the

TABLE 4. Aqueous Humor Parameters Used in Equations 3a and 4

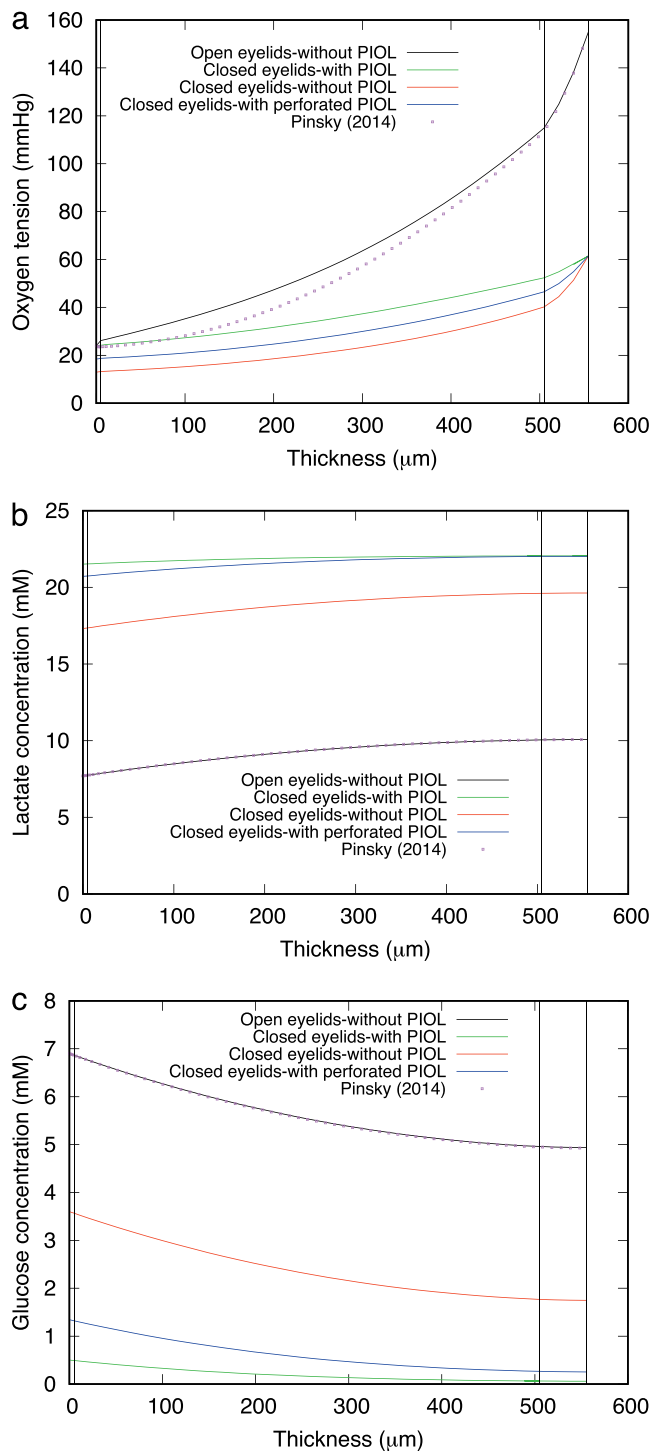| Aqueous Humor Properties			
Density	ρ	1000 kg/m³	
Aqueous inlet flux	Q	1.5 µL/min	McLaren[31]
		$= 2.5 \cdot 10^{-11}$ m³/s	
Kinematic viscosity	v	$7.5 \cdot 10^{-7}$ m²/s	Beswick and McCulloch[32]
Oxygen diffusion coefficient	D_O^{aq}	$2.9 \cdot 10^{-5}$ cm²/s	Chhabra[33]
Glucose diffusion coefficient	D_G^{aq}	$9.3 \cdot 10^{-6}$ cm²/s	Chhabra[33]
Lactate diffusion coefficient	D_L^{aq}	$1.45 \cdot 10^{-5}$ cm²/s	Chhabra[33]

FIGURE 2. Equilibrium oxygen tension (**a**), lactate concentration (**b**), and glucose concentration (**c**) across the thickness of the axis of symmetry of the cornea. The x-axis represents a coordinate in the direction of the anterior pole and with the origin at the interface between the aqueous humor and the corneal endothelium. The *vertical lines* mark the boundaries between the three corneal layers.

aqueous humor and the corneal endothelium. The vertical lines mark the boundaries between the three corneal layers.

Let us consider first the case in which no PIOL is present in the anterior chamber (black and red curves in the figure). Both in the case of open and closed eyelids, moving from epithelium toward the anterior chamber (negative x direction), owing to

oxygen consumption by corneal layers, there is a decline in the oxygen tension. Moreover, since the glucose in our model is solely provided by the aqueous humor and is consumed by the corneal layers, there is a decrease of glucose concentration toward the epithelium. As a consequence of glycolysis, lactate concentration increases toward the epithelium. The results relative to the open eyelids case (black curve) are very similar to what has been predicted by Pinsky[15] (reported with purple dots in Fig. 2).

As discussed above, direct comparison between the two cases has to be considered with care. The reason is that we did not solve for aqueous motion in the case of open eyelids, assuming that the aqueous is well mixed, but we did so in the case of closed eyes (flow streamlines are shown in Fig. 3, right). However, the two cases are likely to be quite different since, in the case of closed eyes, a significant gradient of concentration for all species develops in the anterior chamber, as shown in Figure 4 (right side of each panel). In particular, glucose concentration within the anterior chamber decreases toward the cornea, whereas oxygen and lactate behave oppositely. With our choice for the boundary conditions, oxygen levels in the cornea are significantly lower than when the eyes are closed and the minimum value, which occurs at the endothelium, drops from 24 to ≈13 mm Hg, which is consistent with the experiments of McLaren et al.[21] Glucose concentration at the corneal endothelium is also significantly lower in the case of closed eyelids. We note, not shown here, that this is true even if we impose for glucose concentration at the inlet of the domain the value of 8.3 mM (glucose concentration in blood), which we regard as an upper limit value.

Comparison of the Cases With and Without a PIOL. To better understand the effect of a PIOL in the anterior chamber it is useful to first consider the changes in aqueous flow that are generated by presence of the PIOL. In Figure 3 we present a color map of the velocity magnitude together with streamlines of the flow in the anterior chamber with and without the presence of PIOL. It appears that the PIOL forces fluid toward the periphery of the anterior chamber, and a region of very slow motion forms anteriorly to the PIOL. In this region the flow is characterized by two extremely slow circulations with opposite signs. Since the flow anterior to the lens is slow, glucose in the aqueous has to rely primarily on molecular diffusion in order to reach the central region of the cornea. Since diffusion is a very slow transport mechanism, in this case we expect to find lower levels of glucose along the endothelium. This is confirmed by our results, as shown in Figure 2c (green curve). Indeed, in this case the glucose concentration drops to very low values throughout the thickness of the central cornea. At the posterior apex the glucose concentration drops from 3.5 to 0.5 mM, while at the anterior apex the concentration drops from 1.7 to 0.06 mM. As a consequence of glucose drop, oxygen partial tension in the cornea is higher when the PIOL is present than in the reference case, as shown in Figure 2a.

Figure 4a shows color maps of the steady state glucose concentration in the anterior chamber and cornea, with and without the PIOL. The figure shows that glucose distribution in the two cases is very different. This is essentially due to the advective transport induced by the aqueous motion seen in Figure 3. In the case of an implanted PIOL, fluid is forced toward the periphery of the anterior chamber, leaving a very slow motion anterior to the PIOL. Therefore, glucose levels in the region anterior to the PIOL fall to lower values, in agreement with the results shown in Figure 2c. In Figures 4b and 4c we report color maps of oxygen tension and lactate concentration, for the cases of an anterior chamber with and without the presence of the PIOL, respectively. With the presence of the
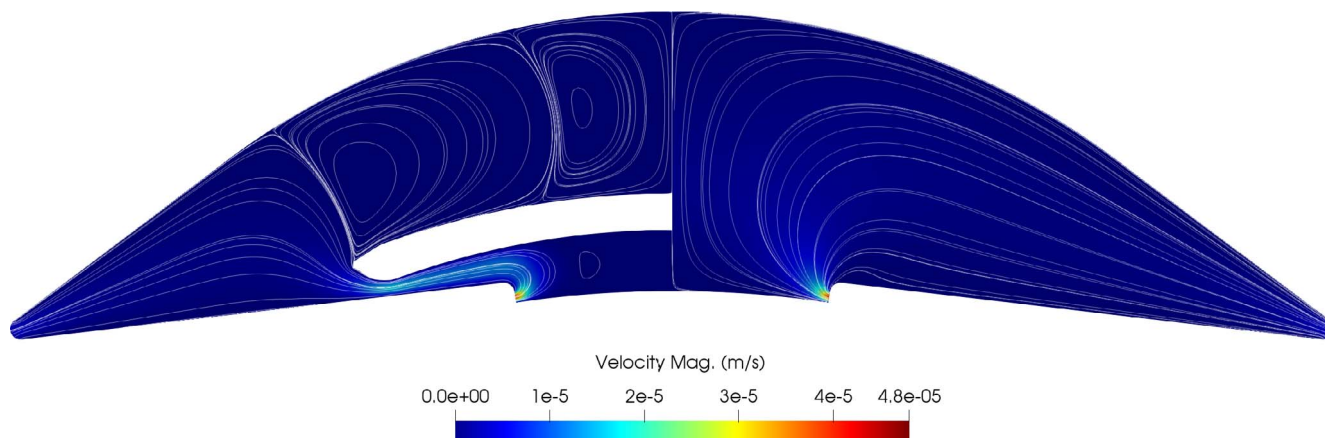
FIGURE 3. Velocity magnitude and flow streamlines in the anterior chamber with (*left*) and without (*right*) PIOL.

PIOL the center of cornea has a lower glucose concentration and a lower consumption of oxygen, leading to an increased oxygen level. Moreover, owing to the lack of glucose (and in spite of the small increase of oxygen tension in the cornea), the production rate of lactate increases in the case of an implanted PIOL, which in turn increases lactate concentration.

Comparison of the Cases With and Without a Hole in the PIOL. When a perforation is present in the center of the PIOL, part of the aqueous flow enters the anterior chamber through the iris-lens channel and flows directly toward the cornea[5] (see Fig. 5). Figure 6a shows color maps of steady state glucose concentration in the anterior chamber and the cornea.
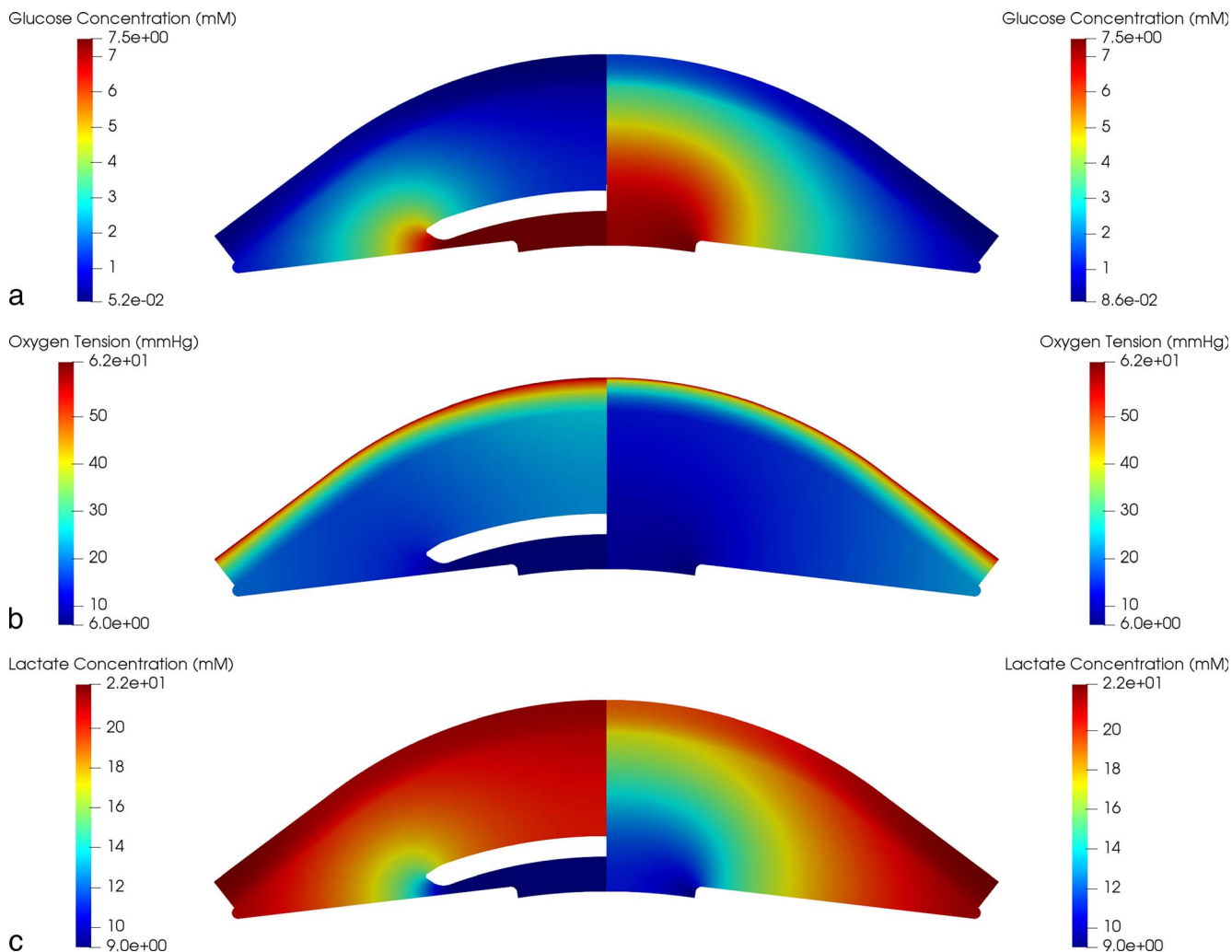

FIGURE 4. Glucose concentration (**a**), oxygen tension (**b**), and lactate concentration (**c**) in the anterior chamber and cornea with (*left*) and without (*right*) PIOL.
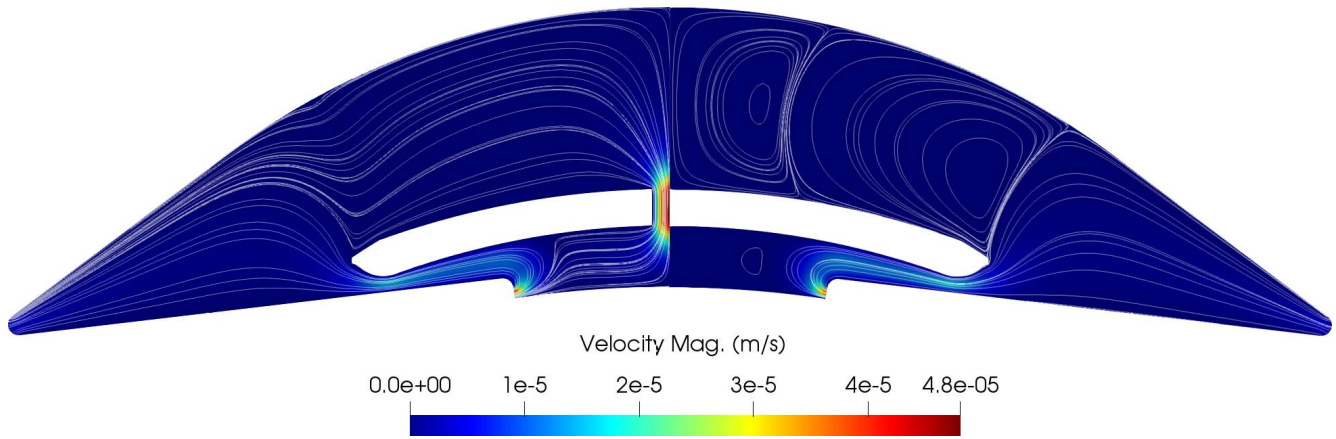
FIGURE 5. Velocity magnitude and flow streamlines in the anterior chamber and cornea with (*left*) and without (*right*) perforation in the PIOL.

As can be seen, considering the advective transport of aqueous flow toward the hole, the availability of glucose at the endothelium is higher than without the perforation. Furthermore, as shown in Figure 2c (blue curve), throughout the corneal layers, the glucose concentration in the presence of the PIOL with a central hole is higher than with the PIOL without any modification, although still much lower than in the case without the PIOL.

Finally, Figures 6b and 6c show color maps of oxygen tension and lactate concentration, respectively. Since oxygen is
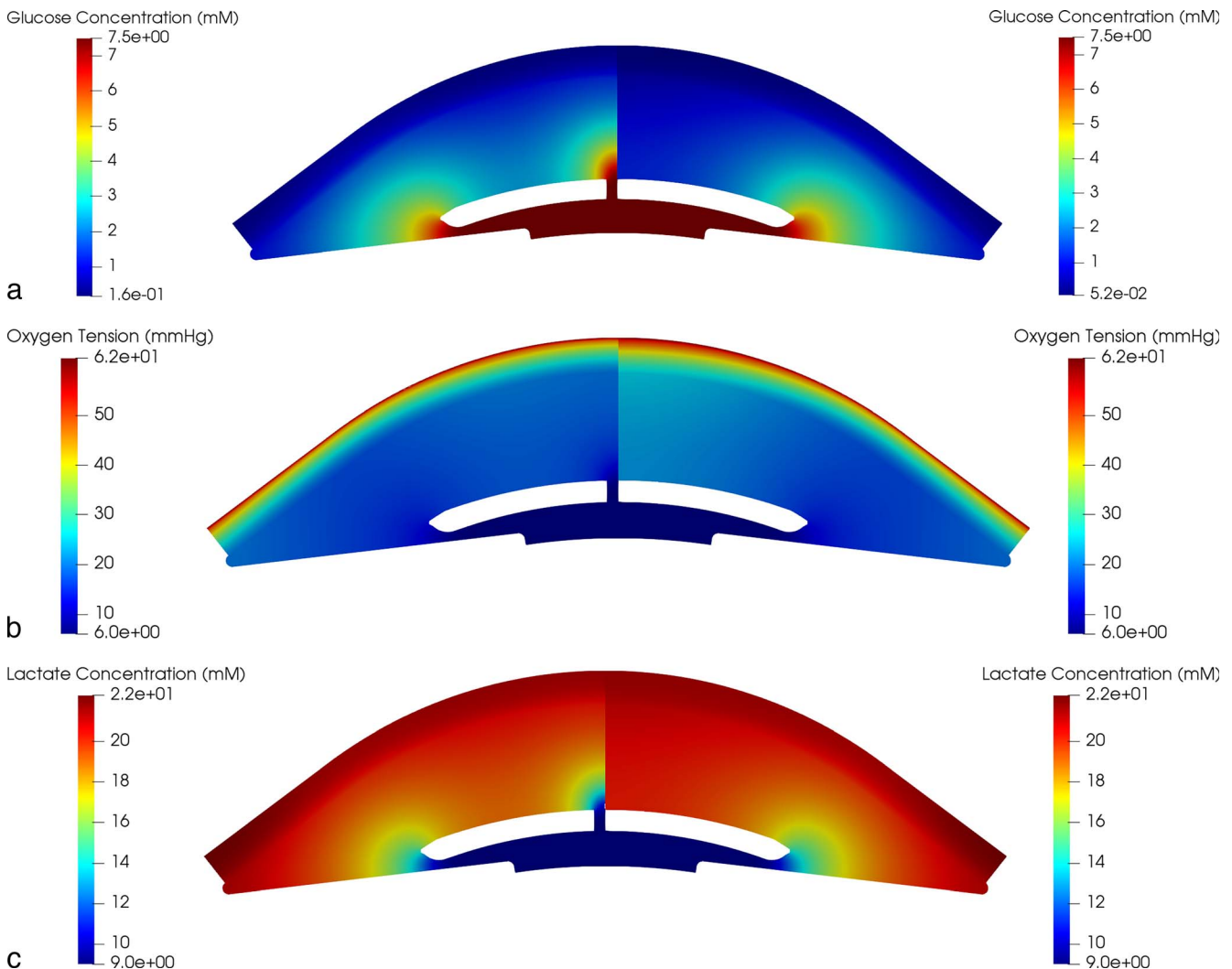

FIGURE 6. Glucose concentration (**a**), oxygen tension (**b**), and lactate concentration (**c**) in the anterior chamber and cornea with a perforated (*left*) and nonperforated (*right*) PIOL.

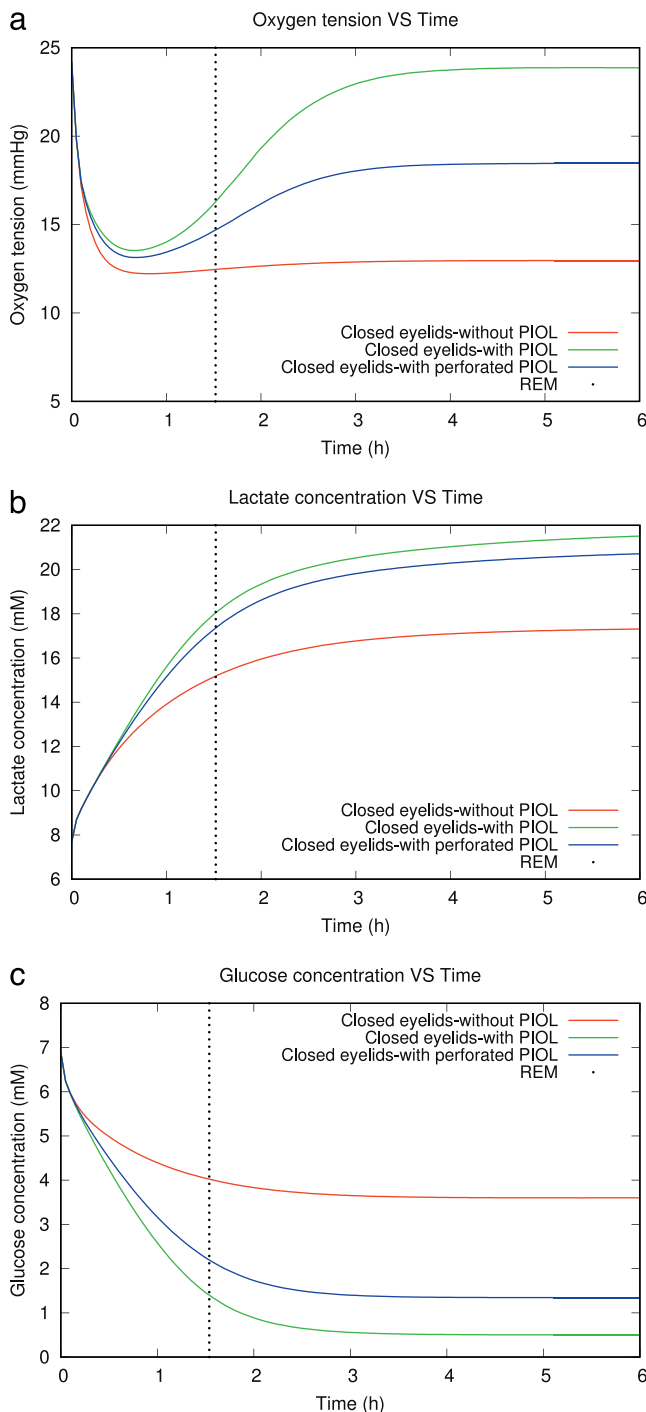Investigative Ophthalmology & Visual Science

FIGURE 7. Time evolution of metabolic species' concentration; oxygen (**a**), lactate (**b**), glucose (**c**), at the center of cornea with and without the PIOL. The *vertical dashed lines* mark the time at which, typically, the first REM occurs. The three curves correspond to the physiological case (*red*), the case of an implanted PIOL (*green*), and the case on an implanted perforated PIOL (*blue*).

Unsteady Simulations

In the previous section we discussed the steady state results of our model. Obviously, for steady state concentrations to be reached a certain time is required, and it is of interest to estimate it. This allows us to verify whether the solutions described in the previous section can be reached in reality. We recall that when eyelids are open it is assumed that the aqueous humor is efficiently mixed by eye rotations and thermal flow. During sleep, these sources of fluid motion are suppressed and fluid motion is generated mainly by production/drainage flow. However, we know that at relatively regular intervals, REMs occur during sleep, which will induce fluid mixing. On average, the first REM phase occurs approximately 90 minutes after falling asleep, during the first sleep cycle. The following REM phases, which are increasingly longer, occur within each sleep cycle, which lasts approximately 1½ hours. Changes of posture during sleep also produce rotations of the eye bulb, which are, however, characterized by low angular velocities and short duration. Thus, they are unlikely to contribute much to fluid mixing.

We assumed that a fully developed production/drainage flow exists in the anterior chamber and we computed the temporal evolution of species' concentrations, imposing values at an initial time corresponding to the open eyelids case. Moreover, we assumed that at the initial time the concentrations of all species in the anterior chamber are uniformly distributed. With these initial conditions we ran unsteady simulations, using the same boundary conditions adopted in the previous section for the case of closed eyelids.

Figure 7 shows the time evolution of the concentration of all species at the anterior chamber–endothelium interface, on the axis of symmetry of the cornea. The red curve corresponds to the case without the PIOL; the green curve, the case in which a PIOL is present; and the blue curve, the case in which the PIOL has a central hole. In this figure we also marked with a vertical dashed black line the time at which the first REM cycle is expected to occur. The figure shows that the time scale of evolution is of the order of some hours: the final steady state is reached in approximately 4 hours. Since the first REM occurs after approximately 90 minutes and successive REMs occur within each sleep cycle, this final steady state is unlikely to be reached in normal conditions.

However, we found that when the first REM phase occurs, the glucose concentration is reduced from 6.9 mM to 4.1 mM (without PIOL), to 2.5 mM (PIOL with hole), and to 1.8 mM (with PIOL).

DISCUSSION AND CONCLUSIONS

We proposed a mathematical model of transport of metabolic species to the cornea, considering the role of aqueous flow in the anterior chamber, which has been neglected in previous works. We considered both the case of open eyelids, when aqueous motion is enhanced by eye rotations and the onset of a thermally induced flow, and closed eyelids, in which case aqueous flow is much less intense. We considered both the physiological case and the case in which a PIOL is implanted in the eye, with the aim of understanding if and to what extent the PIOL affects corneal metabolism.

We accounted for the presence of three species (oxygen, glucose, and lactate) and modeled corneal metabolism, adopting the model proposed by Chhabra et al.,[14] Pinsky,[15] and Alvord et al.,[13] which we suitably modified to better reproduce available experimental data. In particular, we focused on glucose availability at the cornea. This is because oxygen is mostly delivered to the cornea from outside of the

mainly provided from the epithelium side, the central hole in the lens body has a negligible effect in comparison to the case where the PIOL is without a hole. On the other hand, owing to the increase in glucose concentration, anterior to the perforated lens, lactate concentration in this region decreases, which also decreases the risk of corneal acidification.

eye, from the air in the open eyelids condition and from the palpebral circulation in the closed eyelids case. On the other hand, glucose is transported to the cornea by the aqueous humor and its availability at the corneal endothelium is likely to be affected by the presence of an intraocular lens.

Steady state simulations show that the presence of a PIOL has a significant influence on glucose availability on the cornea, in sleep conditions. When a PIOL is implanted, aqueous flow is diverted toward the periphery of the anterior chamber and glucose concentration decreases in the region anterior to the PIOL. However, we showed that several hours are needed for this steady solution to be reached. Since during sleep REMs are expected to occur within every sleep cycle, which occurs every 90 minutes, the steady state solution predicted by our model is unlikely to ever be reached. Rather, the system is constantly in an unsteady state. Glucose concentration anterior to the PIOL progressively decreases until REMs occur; then eye rotations cause mixing of the aqueous humor, and the glucose concentration in front of the PIOL increases again. We found that the minimum value of glucose that is expected to be reached in the presence of a PIOL is approximately half of that corresponding to the nonsurgically altered case, which might be relevant for cell damage (4.1 mM without PIOL and 1.8 mM with PIOL). In the case of a perforated PIOL, glucose and oxygen availability on the cornea increases, compared to the case of a PIOL without a hole, and the lactate concentration correspondingly decreases. It is useful to keep in mind that the duration of the REM depends on age and sleep patterns and may therefore have an influence on glucose availability at the cornea after PIOL implantation. On this basis one could speculate that some people may be at higher risk of corneal endothelial cell damage than others.

Some possibly relevant effects were neglected in the present work, which are worth mentioning. Firstly, we neglected the possible presence of an iridotomy, which is often created when a PIOL is implanted. Iridotomy creates an additional passage from the posterior to the anterior chamber,[6,35] thus modifying fluid flow characteristics in the anterior chamber. We note, however, that iridotomies are typically produced in the periphery of the iris. Thus, the jet of aqueous through the iridotomy enters the anterior chamber close to the trabecular meshwork, where it drains, and is unlikely to significantly contribute to advective transport of nutrients to the central cornea. For this reason we do not think that our conclusions would be qualitatively different, even if the presence of an iridotomy was considered.

We also did not consider the effect of endogenous glycogen in our model. Thus, variations of glucose concentration in the cornea in vivo may not be as strong as predicted by our model.

In summary, we studied the effect of aqueous motion on nutrient transport to the cornea. We compared the physiological case to the case in which an iris-fixated PIOL is implanted in the anterior chamber. Our model suggests that implantation of a PIOL may produce a decrease in nutrient availability in the central region of the cornea during sleep that might be related to the possible loss of endothelial cells. We are unaware of data regarding the physiological threshold of glucose concentration for cell damage, and it must be verified whether our theoretical predictions have clinical relevance.

References

1. Kwitko S, Prestes Stolz A. Iris-claw (artisan®/artiflex®) phakic intraocular lenses for high myopia and high hyperopia. *Expert Rev Ophthalmol*. 2011;6:505–512.

2. Jonker SMR, Berendschot TTJM, Ronden AE, Saelens IEY, Bauer NJC, Nuijts RMMA. Five-year endothelial cell loss after implantation with artiflex myopia and artiflex toric phakic intraocular lenses. *Am J Ophthalmol*. 2018;194:110–119.

3. Chebli S, Rabilloud M, Burillon C, Kocaba V. Corneal endothelial tolerance after iris-fixated phakic intraocular lens implantation: a model to predict endothelial cell survival. *Cornea*. 2018;37:591–595.

4. Repetto R, Pralits JO, Siggers JH, Soleri P. Phakic iris-fixated intraocular lens placement in the anterior chamber: effects on aqueous flowphakic iris-fixated intraocular lens placement. *Invest Ophthalmol Vis Sci*. 2015;56:3061–3068.

5. Davvalo Khongar P, Pralits JO, Soleri P, Repetto R. Aqueous flow in the presence of a perforated iris-fixated intraocular lens. *Meccanica*. 2017;52:577–586.

6. Fernández-Vigo JI, Marcos AC, Agujetas R, et al. Computational simulation of aqueous humour dynamics in the presence of a posterior-chamber versus iris-fixed phakic intraocular lens. *PLoS One*. 2018;13:e0202128.

7. Davvalo Khongar P, Pralits JO, Cheng X, Pinsky P, Soleri P, Repetto R. Effect of an iris-fixated intraocular lens on corneal metabolism: a numerical study. *J Model Ophthalmol*. 2018;2:97–101.

8. Fatt I. Steady-state distribution of oxygen and carbon dioxide in the in vivo cornea: I, the open eye in nitrogen and the covered eye. *Exp Eye Res*. 1968;7:413–430.

9. Fatt I, Bieber MT. The steady-state distribution of oxygen and carbon dioxide in the in vivo cornea: I, the open eye in air and the closed eye. *Exp Eye Res*. 1968;7:103–112.

10. Canning CR, Greaney MJ, Dewynne JN, Fitt A. Fluid flow in the anterior chamber of a human eye. *IMA J Math Appl Med Biol*. 2002;19:31–60.

11. Abouali O, Modareszadeh A, Ghaffarieh A, Tu J. Investigation of saccadic eye movement effects on the fluid dynamic in the anterior chamber. *J Biomech Eng*. 2012;134:021002.

12. Dvoriashyna M, Repetto R, Tweedy JH. Oscillatory and steady streaming flow in the anterior chamber of the moving eye. *J Fluid Mech*. 2019;863:904–926.

13. Alvord LA, Hall WJ, Keyes LD, Morgan CF, Winterton LC. Corneal oxygen distribution with contact lens wear. *Cornea*. 2007;26:654–664.

14. Chhabra M, Prausnitz JM, Radke CJ. Modeling corneal metabolism and oxygen transport during contact lens wear. *Optom Vis Sci*. 2009;86:454–466.

15. Pinsky PM. Three-dimensional modeling of metabolic species transport in the cornea with a hydrogel intrastromal inlay3d modeling of metabolic species transport. *Invest Ophthalmol Vis Sci*. 2014;55:3093–3106.

16. Cheng X, Pinsky PM. A numerical model for metabolism, metabolite transport and edema in the human cornea. *Comput Methods Appl Mech Eng*. 2017;314:323–344.

17. Takahashi GH, Fatt I. The diffusion of oxygen in the cornea. *Exp Eye Res*. 1965;4:4–12.

18. Bonanno JA, Polse KA. Corneal acidosis during contact lens wear: effects of hypoxia and CO2. *Invest Ophthalmol Vis Sci*. 1987;28:1514–1520.

19. Ruben CM, Zhu YY. Occlusion of the cornea with contact lens and anterior chamber lactate levels. *Acta Ophthalmol*. 1987;65:287–292.

20. Harvitt DM, Bonanno JH. pH dependence of corneal oxygen consumption. *Invest Ophthalmol Vis Sci*. 1998;39:2778–2781.

21. McLaren JW, Dinslage S, Dillon JP, Roberts JE, Brubaker RF. Measuring oxygen tension in the anterior chamber of rabbits. *Invest Ophthalmol Vis Sci*. 1998;39:1899–1909.

22. Fatt I, Weissman BA. *Physiology of the Eye: An Introduction to the Vegetative Functions*. Stoneham, Massachusetts: Butterworth-Heinemann; 2013.

23. Riley MV. Glucose and oxygen utilization by the rabbit cornea. *Exp Eye Res*. 1969;8:193–200.

24. Freeman RD. Oxygen consumption by the component layers of the cornea. *J Physiol*. 1972;225:15–32.

25. Leung BK, Bonanno JA, Radke CJ. Oxygen-deficient metabolism and corneal edema. *Prog Retin Eye Res*. 2011;30:471–492.

26. Bonanno JA, Stickel T, Nguyen T, et al. Estimation of human corneal oxygen consumption by noninvasive measurement of tear oxygen tension while wearing hydrogel lenses. *Invest Ophthalmol Vis Sci*. 2002;43:371–376.

27. von Helmholtz H. *Handbuch der physiologischen Optik*. 3rd ed. Arbor, Ann MI: University of Michigan Library; 1909.

28. Fernández-Vigo JI, Macarro-Merino A, Fernández-Francos J, et al. Computational study of aqueous humor dynamics assessing the vault and the pupil diameter in two posterior-chamber phakic lenses. *Invest Ophthalmol Vis Sci*. 2016;57:4625–4631.

29. Riley MV. Intraocular dynamics of lactic acid in the rabbit. *Invest Ophthalmol Vis Sci*. 1972;11:600–607.

30. Davson H. *Physiology of the Eye*. London, United Kingdom: Macmillan Education UK; 1990.

31. McLaren JW. Measurement of aqueous humor flow. *Exp Eye Res*. 2009;88:641–647.

32. Beswick JA, McCulloch C. Effect of hyaluronidase on the viscosity of the aqueous humour. *Br J Ophthalmol*. 1956;40:545–548.

33. Chhabra M. *Oxygen Transport Through Soft Contact Lens and Cornea: Lens Characterization and Metabolic Modeling*. Berkeley, California: ProQuest; 2007.

34. Nau CB, Malihi M, McLaren JW, Hodge DO, Sit AJ. Circadian variation of aqueous humor dynamics in older healthy adults. *Invest Ophthalmol Vis Sci*. 2013;54:7623–7629.

35. Dvoriashyna M, Repetto R, Romano MR, Tweedy JH. Aqueous humour flow in the posterior chamber of the eye and its modifications due to pupillary block and iridotomy. *Math Med Biol*. 2018;35:447–467.